Magnetically induced variations in phonon frequencies

Joo-Hyoung Lee, Young-Chung Hsue, and Arthur J. Freeman

Department of Physics and Astronomy, Northwestern University, Evanston, Illinois 60208, USA

The long-standing question of the existence of phonon-magnetism interactions in metals is examined from first principles. Through density-functional-based linear-response calculations, we show that the phonon frequencies of fcc Ni have an explicit and appreciable dependence on its magnetic moment: the frequencies increase with the magnetic moment near the Brillouin zone center, whereas the situation becomes reversed near the zone boundary, and this behavior originates from the combined role of the spin-dependent screening due to the electrons and the effect of magnetostriction.

The fundamental physics of metallic magnetism has not been satisfactorily understood as yet and continues to be a highly active field of research both theoretically and experimentally. On the theoretical side, recent efforts have been focused on the correct description of observed quantities such as Curie temperature and magnon spectra,[1] while experimental studies show the large variety and complexity of materials whose magnetic properties can be investigated with today's techniques. Manganites,[2] ruthenates,[3] and even high-T_C superconductors[4] are a few examples. However, all these studies are mainly focused on the electronic and charge degrees of freedom; although an important constituent of solids, the phononic one has not been seriously taken into account in magnetism research.

The challenging question as to the possible interaction of magnetism and phonons in metals, raised in the work of Kim,[5,6] has been answered relatively recently by several experiments: Raman scattering experiments on the metallic oxide $SrRuO_3$ (Ref. 7) revealed an anomalous softening of the optical phonons and a phonon linewidth that is strongly affected by the ferromagnetic transition near $T_C \sim 150$ K. In addition, Raman scattering on half-metallic CrO_2 (Ref. 8) in an external magnetic field showed that the frequency of the E_g phonon mode dramatically increases with increasing magnetic field. While the origins of these anomalies were attributed to the reorganization of the electronic band structure[7] and a spin-phonon coupling,[8] respectively, no quantitative analysis was made, and the detailed mechanism of the coupling has yet to be understood. In developing his theory, Kim performed intensive studies on the magnetism-phonon interaction using the electron gas model and linear-response theory. Among the important predictions are[5,6] (i) the phonon frequencies in ferromagnetic metals show a dependence on the magnetic moment through spin-dependent electronic screening, (ii) thus the sound velocity, which is experimentally measured, becomes also magnetically dependent, and (iii) the magnetization can also be affected by phononic contributions.

In this Brief Report, we present results of a systematic first-principles study of the phonon dispersions of fcc Ni with variation of its magnetic moment. To this end, we used a combined density-functional perturbation theory (DFPT)[9] and fixed spin moment (FSM) method.[10] Nickel is selected because it is one of the ferromagnetic elements with a simple lattice and electronic structure, which alleviates the compu-

tational workload in phonon calculations and simplifies the interpretation of the results obtained. Our first-principles calculations reveal that due to the interplay between the electronic screening and the magnetostriction, the phonon frequencies of Ni show an appreciable change as its magnetic moment varies. We expect that these results will serve as a first step in advancing research and understanding of this newly reexplored area of magnetism.

All calculations were performed with the highly precise all-electron full-potential linearized augmented plane wave (FLAPW) method;[15] for the **k**-point integrations, 408 irreducible **k** points generated by the Monkhorst-Pack scheme[16] are used with a Gaussian broadening parameter of 0.027 eV. The muffin-tin (MT) radius and plane-wave cutoff are chosen to be 2.15 a.u. and 13.69 Ry, respectively. The core electrons and valence electrons are treated fully and scalar relativistically, respectively. The charge density and potential are represented in terms of lattice harmonics with $l_{max}=8$ inside the MT sphere, and the local-density approximation (LDA)[17] is employed for the exchange-correlation potential.[18] We first determine the equilibrium properties from a fit with the Murnaghan equation of state, which are shown in Table I. The results with the generalized gradient approximation (GGA) are given for comparison purposes. As is usual, LDA underestimates the lattice constant (−2.4% in this case) compared to experiment, whereas the GGA gives a better agreement with a −0.2% discrepancy. For the spin magnetic moment, LDA (+3.3%) gives a better agreement with experiment (which includes a small orbital moment, $\mu_{orb}=0.055\mu_B$) than does the GGA (+6.2%).

To calculate the phonon frequencies, we employed DFPT, which is implemented with the FLAPW method,[19] and as in the equilibrium calculations all electrons are taken into account to calculate the full-potential contribution using the

TABLE I. Calculated lattice constant a, bulk modulus B, and magnetic moment μ of fcc Ni. The results with GGA[11] are given for comparison.

	LDA	GGA	Expt.
a (a.u.)	6.49	6.64	6.65 (Ref. 12)
B (Mbar)	2.51	2.05	1.90 (Ref. 13)
μ (μ_B)	0.63	0.66	0.61 (Ref. 14)
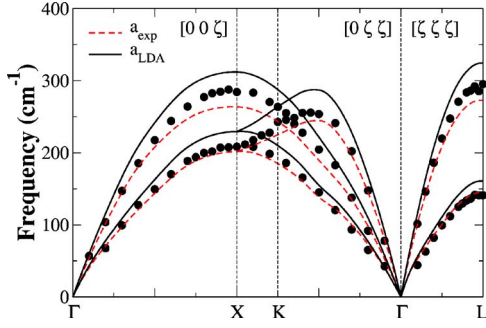
FIG. 1. (Color online) Calculated phonon dispersions of fcc Ni along high-symmetry lines both at the LDA lattice constant (black solid lines) and at the experimental one (red dashed lines). Experimental data (circles)[21] are given for comparison.

pseudocharge approach of Weinert.[20] Phonon frequencies are calculated at eight phonon vectors along each of three high-symmetry directions, $\Gamma \rightarrow L$, $\Gamma \rightarrow X$, and $\Gamma \rightarrow K \rightarrow X$, and the full dispersions are obtained through interpolation. Convergence of the calculated phonon frequencies with the number of **k** points has been carefully checked and 408 **k** points in the irreducible Brillouin zone (IBZ) were found to be sufficient.

First, we calculated the phonon dispersions of fcc Ni at its equilibrium volume, and the results are shown in Fig. 1 along with inelastic neutron scattering data at $T=296$ K (Ref. 21) for comparison. The calculations were performed both at the LDA lattice constant and at the experimental one. As is clear from the figure, the LDA lattice constant overestimates the frequency with a maximum difference of 29.24 cm^{-1} (+10.0%) for the longitudinal mode at the L point, whereas the use of the experimental lattice constant, which is larger than the LDA value, significantly corrects the overestimation, giving overall a better agreement with experiment. This implies that the phonon frequencies of fcc Ni depend rather sensitively on the lattice constant. We note that the same frequency overestimation at the LDA lattice constant was found in other calculations[22] and attributed to the overbinding of the LDA. It should be noted that the effect of temperature has not been taken into account in comparing with experiment. Since the lattice constant increases with temperature due to an anharmonic effect, a better agreement with experiment is expected if an increase in the lattice constant due to the temperature effect is properly taken into account.[22]

Now, in order to investigate the effect of magnetism on the phonon frequencies, we calculated the phonon dispersions at three other magnetic moments, $\mu=0.0$, 0.3, and $1.0\mu_B$, using the FSM method. For each magnetic moment, the new equilibrium lattice constant is found through total energy calculations, and the results are listed in Table II, in which the last column, $\Delta=[a(\mu)-a(\mu_{opt})]/a(\mu_{opt})$ with $\mu_{opt}=0.63\mu_B$, represents the relative difference in the lattice constants. As one can see from Table II, the lattice constant increases slightly with the magnetic moment, which is interpreted as a high-field magnetostriction resulting from an increase of the spontaneous magnetization.[23] Note that due to this increase, the phonon frequencies would be expected to decrease as the magnetic moment increases. The phonon dis-

TABLE II. Equilibrium lattice constant a at each magnetic moment of Ni and its relative difference (in percent) from the optimized moment value.

μ (μ_B)	a (a.u.)	Δ
0.0	6.456	−0.54%
0.3	6.458	−0.52%
0.63 ($\equiv\mu_{opt}$)	6.492	
1.0	6.504	0.18%

persions, which were calculated at each equilibrium lattice constant for different magnetic moments with the magnetic moment fixed at the desired value (referred to as case I), are presented in Fig. 2.

As is clear from the figure, an appreciable change occurs in the dispersions as the magnetic moment varies. In order to examine the changes in the frequencies in more detail, we calculated the frequency differences, $\Delta\nu=\nu(\mu)-\nu(\mu_{opt})$, where ν is the phonon frequency, and plotted the result along $\Gamma \rightarrow K \rightarrow X$ in Figs. 3(a)–3(c). The first thing to note from Fig. 3 is that $|\Delta\nu| \lesssim 15$ cm^{-1} in all cases [including $\Gamma \rightarrow L$ and $\Gamma \rightarrow X$ (Ref. 24)] except for the lower transverse mode of the spin-unpolarized case, for which $|\Delta\nu| \sim 23$ cm^{-1} around $(a/2\pi)\mathbf{q} \sim (0,0.35,0.35)$ [Fig. 3(a)]. The calculated changes here can be compared with the observed changes in the above-mentioned experiments on SrRuO$_3$ and CrO$_2$, in which the frequency changes were found to be less than 10 cm^{-1} as the sample magnetization changes.[7,8] Thus, the frequency changes calculated in the present work imply that the magnetic effect on the frequencies is not small for fcc Ni—unlike the conclusion of other work,[22] in which comparison was made between spin-polarized and unpolarized cases only.

Another characteristic from Fig. 3 is that the frequencies with smaller magnetic moments than μ_{opt} are smaller than $\nu(\mu_{opt})$ up to a certain **q** vector, and become larger than $\nu(\mu_{opt})$ afterwards; the frequency for the magnetic moment larger than μ_{opt} is larger than $\nu(\mu_{opt})$ up to some **q** vector, and becomes smaller than $\nu(\mu_{opt})$ after that. Also, the frequency difference between $\mu=0.0$ and $0.3\mu_B$ is smaller than other cases due to the closeness in their lattice constants, and
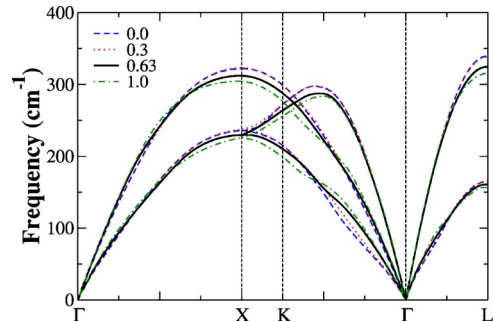
FIG. 2. (Color online) Phonon dispersions at $\mu=0.0$ (blue dashed), 0.3 (red dotted), 0.63 (black solid) and $1.0\mu_B$ (green dot-dashed) at each equilibrium lattice constant for different magnetic moments.
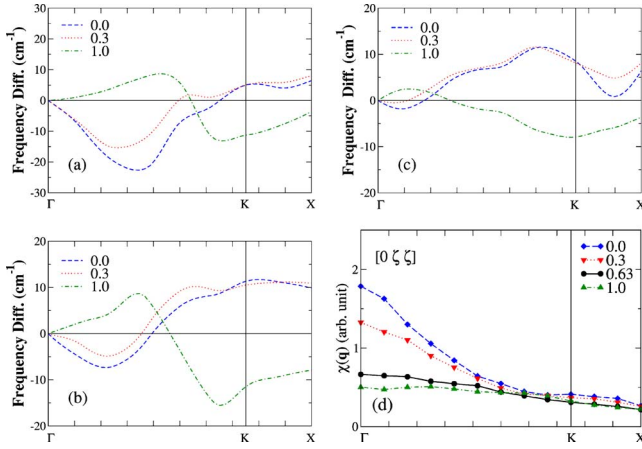
FIG. 3. (Color online) $\Delta\nu$ at the optimized lattice constant for each magnetic moment in the (a) lower transverse, (b) upper transverse, and (c) longitudinal mode along $\Gamma\rightarrow K\rightarrow X$, and (d) the corresponding $\chi_\mu(\mathbf{q})$.

it becomes further reduced ($\lesssim 2$ cm^{-1}) as the zone boundary is approached. We note that this characteristic is common in all directions;[24] the origin of the anomalous dip for $\mu=0.0\mu_B$ near the X point in the longitudinal mode is unclear.

To understand the origin of the calculated μ dependence of the frequencies, we calculated the phonon dispersions and frequency differences, $\Delta\nu$, at the optimized LDA lattice constant $a(\mu_{\mathrm{opt}})=6.492$ a.u., which is larger than $a(\mu)$ for $\mu=0.0$ and $0.3\mu_B$ and smaller than that for $\mu=1.0\mu_B$, for all magnetic moments considered (referred to as case II). The $\Delta\nu$'s are given in Figs. 4(a)–4(c) along $\Gamma\rightarrow K\rightarrow X$.

Comparison of Fig. 3 with Fig. 4 shows that for $\mu=0.0$ and $0.3\mu_B$, the frequency difference in case II remains almost the same as that of case I near the center and in the middle of the zone; the frequencies for these magnetic moments in case II are slightly less than those in case I with the maximum difference of 3 cm^{-1}. Similarly, the frequencies for $\mu=1.0\mu_B$ in case II change very little compared to those of case I except for the longitudinal case for which the maximum increase of 3 cm^{-1} occurs around $(a/2\pi)\mathbf{q}\sim(0,0.44,$
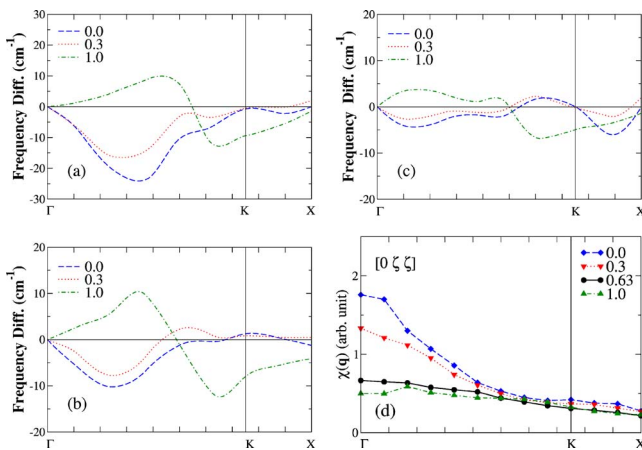
FIG. 4. (Color online) $\Delta\nu$ at the fixed lattice constant for all magnetic moments in the (a) lower transverse, (b) upper transverse, and (c) longitudinal mode along $\Gamma\rightarrow K\rightarrow X$, and (d) the corresponding $\chi_\mu(\mathbf{q})$.
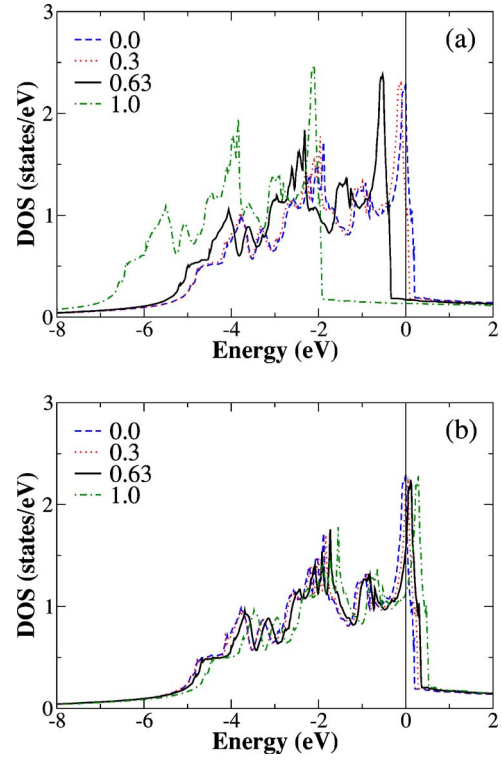
FIG. 5. (Color online) Density of states of fcc Ni for (a) spin-up and (b) spin-down.

0.44). Near the zone boundary, however, the frequencies for $\mu=0.0$ and $0.3\mu_B$ in case I are larger by up to 11 cm^{-1} than those in case II, and the frequencies for $\mu=1.0\mu_B$ in case I are smaller than those in case II by up to 3.7 cm^{-1}.

This comparison shows that although the magnetostriction in Table II has the anticipated effect near the zone boundary, the smaller frequencies for the larger lattice constants, the frequency behavior is exactly opposite to the above expectation near the zone center. This behavior can be understood from the magnetic dependence of the electronic screening, which is determined by the electronic structure of Ni.

In his work, Kim proposed the fully screened phonon frequency in a metal as[5]

$$\omega^2(\mathbf{q}) = \Omega^2(\mathbf{q}) - |g(\mathbf{q})|^2 \chi_\mu(\mathbf{q},\omega(\mathbf{q})), \qquad (1)$$

where $\Omega(\mathbf{q})$ is the bare phonon frequency, $\omega(\mathbf{q})$ the frequency fully screened by the conduction electrons, $g(\mathbf{q})$ the electron-phonon matrix element,[25] and $\chi_\mu(\mathbf{q},\omega(\mathbf{q}))$ represents the electron polarizability, which describes the electronic screening. Here, we first note that since the electrons respond to the nuclear motion instantaneously due to the large mass ratio (the so-called "adiabatic approximation"), $\chi_\mu(\mathbf{q},\omega(\mathbf{q}))$ can be approximated as $\chi_\mu(\mathbf{q})$. Extending the results from the random phase approximation (RPA),[26] we obtain for the spin-polarized cases

$$\chi_\mu(\mathbf{q}) \simeq \frac{1}{V}\sum_\sigma \sum_{\mathbf{k},n} \left[\sum_m{}' \frac{f(\varepsilon_{n\mathbf{k}}^\sigma) - f(\varepsilon_{m\mathbf{k}+\mathbf{q}}^\sigma)}{\varepsilon_{m\mathbf{k}+\mathbf{q}}^\sigma - \varepsilon_{n\mathbf{k}}^\sigma} M_{m\mathbf{k}+\mathbf{q},n\mathbf{k}}^\sigma \right.$$
$$\left. + \sum_m{}'' \delta(\varepsilon_F^\sigma - \varepsilon_{n\mathbf{k}}^\sigma) M_{m\mathbf{k}+\mathbf{q},n\mathbf{k}}^\sigma \right], \qquad (2)$$

where $M_{m\mathbf{k}+\mathbf{q},n\mathbf{k}}^\sigma = |\langle\psi_{m\mathbf{k}+\mathbf{q}}^\sigma|e^{i\mathbf{q}\cdot\mathbf{r}}|\psi_{n\mathbf{k}}^\sigma\rangle|^2$, V is a crystal volume,

ε_F^σ is the Fermi energy for a spin σ, and $f(\varepsilon_{n\mathbf{k}}^\sigma)$ and $\psi_{n\mathbf{k}}^\sigma$ are the occupation function (1 for $\varepsilon_{n\mathbf{k}}^\sigma \leq \varepsilon_F^\sigma$ and 0 otherwise at $T=0$) and Kohn-Sham orbital of the $n\mathbf{k}$ state with a spin σ and Kohn-Sham eigenvalue $\varepsilon_{n\mathbf{k}}^\sigma$, respectively. In Σ_m', the bands with $\varepsilon_{m\mathbf{k+q}}^\sigma = \varepsilon_{n\mathbf{k}}^\sigma$ are excluded, and Σ_m'' represents the sum over the bands with $\varepsilon_{m\mathbf{k+q}}^\sigma = \varepsilon_{n\mathbf{k}}^\sigma$ only. In Eq. (2), local field effects and higher-order correction terms are neglected.

The calculated $\chi_\mu(\mathbf{q})$ using Eq. (2) along $\Gamma \to K \to X$ for the various magnetic moments at the μ-optimized and the fixed lattice constants are shown in Fig. 3(d) and Fig. 4(d), respectively. As is clear from these figures, while the electron polarizability does not change with the lattice constant very much, it shows a large dependence on the magnetization: $\chi_\mu(\mathbf{q})$ is greatly suppressed up to by a factor of 3.5 as μ increases near the zone center, and the difference in $\chi_\mu(\mathbf{q})$ among the different μ's becomes very small as the zone boundary is approached. The suppression of $\chi_\mu(\mathbf{q})$ as μ increases can be understood from the density of states (DOS) of Ni, which are presented in Fig. 5 for spin-up and spin-down separately. As one can see from Fig. 5(a), almost all states for spin-up are rapidly occupied as μ increases. Due to this almost-full occupation for $\mu=0.63$ and $1.0\mu_B$, the function to be summed in the first term of Eq. (2) becomes very small for spin-up and so does the spin-up component $\chi_\uparrow(\mathbf{q})$. For spin-down, however, the situation is different [Fig. 5(b)]: as μ increases, the Fermi level goes down but the shift in the Fermi level is not as significant as in the spin-up case. As a result, there still remain appreciable portions of the unoccupied states, which are relatively close to each other for different magnetic moments, and thus $\chi_\downarrow(\mathbf{q})$ does not change as much as does $\chi_\uparrow(\mathbf{q})$. We note that the frequency change in Ni can be observed by a similar experiment as that in Ref. 27 because Ni is known as an itinerant (Stoner) ferromagnet.[27]

Another system of interest which may show a large coupling between phonons and magnetism is Invar alloys such as Fe-Ni:[28] As the volume of an Invar remains almost constant below T_C, the frequency variation is expected to come only from the change in the electronic screening for which the magnetic effect on phonon frequencies is large when the Fermi level of one spin channel shifts more rapidly than does that of the other spin. Since this is expected to occur for an Fe-Ni alloy,[29] the phonon frequency may show a large magnetic effect in these materials. We also note that just as the magnetization affects the phonon frequency, the magnetization can be affected by phononic contributions as derived by Kim,[6] which implies that the phonons and magnetization need to be determined in a self-consistent way. Thus, the present work is expected to stimulate more investigations in these directions as well.

[1] S. V. Halilov, H. Eschrig, A. Y. Perlov, and P. M. Oppeneer, Phys. Rev. B **58**, 293 (1998); J. Kübler, *ibid.* **67**, 220403(R) (2003).

[2] N. A. Babushkina *et al.*, Nature (London) **391**, 159 (1998); A. Anane *et al.*, Phys. Rev. B **59**, 77 (1999); C. P. Adams *et al.*, *ibid.* **70**, 134414 (2004).

[3] L. Klein *et al.*, Phys. Rev. Lett. **77**, 2774 (1996); J. C. Jiang *et al.*, Appl. Phys. Lett. **72**, 2963 (1998); N. Kikugawa C. Bergemann, A. P. Mackenzie, and Y. Maeno, Phys. Rev. B **70**, 134520 (2004).

[4] E. W. Hudson *et al.*, Nature (London) **411**, 920 (2001); B. Lake *et al.*, *ibid.* **415**, 299 (2002).

[5] D. J. Kim, J. Phys. Soc. Jpn. **40**, 1244 (1976); **40**, 1250 (1976).

[6] D. J. Kim, Phys. Rev. B **25**, 6919 (1982).

[7] D. Kirillov *et al.*, Phys. Rev. B **51**, 12825 (1995); M. N. Iliev *et al.*, *ibid.* **59**, 364 (1999).

[8] T. Yu *et al.*, J. Phys.: Condens. Matter **15**, L213 (2003).

[9] S. Baroni, P. Giannozzi, and A. Testa, Phys. Rev. Lett. **58**, 1861 (1987); R. Yu and H. Krakauer, Phys. Rev. B **49**, 4467 (1994); S. Baroni *et al.*, Rev. Mod. Phys. **73**, 515 (2001).

[10] V. L. Moruzzi and P. M. Marcus, Phys. Rev. B **42**, 8361 (1990), and references therein.

[11] J. P. Perdew, K. Burke, and M. Ernzerhof, Phys. Rev. Lett. **77**, 3865 (1996).

[12] N. W. Ashcroft and N. D. Mermin, *Solid State Physics* (Saunders College Publishing, Philadelphia, 1976).

[13] K. Gschneidner, *Solid State Physics* (Academic, New York, 1964), Vol. 16.

[14] C. Kittel, *Introduction to Solid State Physics*, 7th ed. (Wiley, New York, 1996).

[15] E. Wimmer, H. Krakauer, M. Weinert, and A. J. Freeman, Phys. Rev. B **24**, 864 (1981); H. J. F. Jansen and A. J. Freeman, *ibid.* **30**, 561 (1984).

[16] H. J. Monkhorst and J. D. Pack, Phys. Rev. B **13**, 5188 (1976).

[17] U. von Barh and L. Hedin, J. Phys. C **5**, 1629 (1972).

[18] The use of the GGA lattice constant (which is better than the LDA one) in a full LDA phonon frequency calculation will yield the same results as does a full GGA phonon calculation [D. L. Novikov and N. E. Christensen (unpublished)].

[19] J.-H. Lee, Ph.D. thesis, Northwestern University, 2005.

[20] M. Weinert, J. Math. Phys. **22**, 2433 (1981).

[21] R. J. Birgeneau *et al.*, Phys. Rev. **136**, A1359 (1964).

[22] A. Dal Corso and S. de Gironcoli, Phys. Rev. B **62**, 273 (2000).

[23] E. W. Lee, Rep. Prog. Phys. **18**, 184 (1955).

[24] J.-H. Lee, Y.-C. Hsue, and A. J. Freeman (unpublished).

[25] Note that $\Omega(\mathbf{q})$ and $g(\mathbf{q})$ do not depend on μ; $\Omega(\mathbf{q})$ is determined solely from the bare internuclear interaction, and since the basis for the underlying Hamiltonian (Ref. 5) is a Bloch function multiplied by a Pauli spin matrix, in calculating $g(\mathbf{q})$ the Pauli spin matrices are dropped out and $g(\mathbf{q})$ becomes spin-independent.

[26] S. L. Adler, Phys. Rev. **129**, 413 (1962); N. Wiser, *ibid.* **129**, 62 (1963).

[27] T. J. Kreutz, T. Greber, P. Aebi, and J. Osterwalder, Phys. Rev. B **58**, 1300 (1998).

[28] M. Hayase, M. Shiga, and Y. Nakamura, J. Phys. Soc. Jpn. **34**, 925 (1973).

[29] P. James, O. Eriksson, B. Johansson, and I. A. Abrikosov, Phys. Rev. B **59**, 419 (1999).